JCTC Journal of Chemical Theory and Computation

Valence Excited States in Large Molecules via Local Multireference Singles and Doubles Configuration Interaction

Tsz S. Chwee[†] and Emily A. Carter*[,‡]

Departments of Chemistry and Mechanical and Aerospace Engineering and the Program in Applied and Computational Mathematics, Princeton University, Princeton, New Jersey 08544-5263, United States

Received August 25, 2010

Abstract: We demonstrate that valence excited states in large molecules can be treated using local multireference singles and doubles configuration interaction (LMRSDCI). The interior eigenvalues corresponding to the excited states of interest are transformed and shifted to the extrema of the spectrum by way of oblique projections and a matrix shift within a modified Davidson diagonalization scheme. In this way, the approximate wave function associated with the excited state of interest can be isolated independently of the lower lying roots, and residual minimization is used for final convergence to the target eigenstate. We find that vertical excitation energies calculated using LMRSDCI are mostly within 0.2 eV of nonlocal MRSDCI values.

1. Introduction

The characterization of molecules in their electronically excited states finds relevance in many areas and applications ranging from the study of photophysical and photochemical processes in molecules to the development of solar cells in material science. For instance, there is considerable interest in the photophysical behavior of nucleic acid bases such as cytosine and thymine when exposed to ultraviolet radiation, as the resulting DNA damage may have cytotoxic/genotoxic consequences.[1,2] Separately, insight into chemical dynamics may rely on characterization of optically dark states that are inaccessible to photoexcitation/photoabsorption studies. While complementary techniques such as electron impact methods may be used to probe such states, they are impeded by inherently low resolution. As such, theoretical methods with capabilities beyond the characterization of the electronic ground state are important tools in aiding the understanding of the above-mentioned phenomena.

Indeed, many of the *ab initio* electronic structure methods commonly used to study molecules in the electronic ground state can be adapted for excited states. For example, in the method of configuration interaction singles (CIS), the CI Hamiltonian is diagonalized in the basis of singly excited determinants, and the higher roots serve as approximations to the excited states. Due to the lack of electron correlation, the quality of CIS calculations for the excited states is similar to that of Hartree−Fock (HF) for the ground state. Nevertheless, it has formed the basis for further improvements such as the inclusion of a perturbative doubles correction (CIS(D)),[3,4] spin-flip CIS,[5] and different variants of the XCIS[6,7] implementation.

Among methods that incorporate the effects of electron correlation, time-dependent DFT (TDDFT)[8,9] is one of the most computationally affordable. The foundation for extending conventional, time-independent DFT into the time domain is based on the Runge−Gross theorem,[8] which states the existence of a unique mapping between the time-dependent external potential and the density of a system. The relatively low cost of TDDFT computations facilitates the study of larger molecules than possible with other approaches, although there are well documented limitations with using this approach to study (i) Rydberg-type excitations, (ii) multielectron excitations, and (iii) excitations involving charge transfer.[10−13] Nevertheless, there has been progress in describing long-range charge-transfer excitations within DFT by imposing constraints (e.g., charge differences between the donor and acceptor fragments) within the ground

* Corresponding author e-mail: eac@princeton.edu.

[†] Department of Chemistry.

[‡] Department of Mechanical and Aerospace Engineering and the Program in Applied and Computational Mathematics.

10.1021/ct100486q
Published on Web 12/03/2010

state formalism. The dominant Coulombic interaction between the charge transfer fragments can be correctly modeled using this approach.[14−16]

Within the domain of single-determinant-based wave function approaches, methods based on coupled cluster theory (CC) have been used extensively for studying excited states in small to medium sized molecules. Provided that the HF wave function serves as a good reference for the ground state and the excited states are single configurational in character, low order CC-based approaches such as equation-of-motion CC (EOM-CC)[17,18] and the closely related linear-response CC (LR-CC)[19−21] are among the most accurate approaches for treating singly excited states, yielding excitation energies within 0.3 eV of experimental values. While full EOM-CC and LR-CC are formally suitable for treating all excited states, current practical implementations of EOM-CC and LR-CC include up to the triple excitation cluster operator, i.e., CCSDT,[22,23] which scales as $O(N^8)$; higher order formulations such as CCSDTQ[24,25] are too expensive apart from benchmarking purposes. To reduce the cost associated with the family of CC methods, various approximations have been introduced. For example, in the method of CC2,[26] all terms in the $\hat{T}_2$ equations higher than second-order are neglected, reducing the overall computational cost to $O(N^5)$ from $O(N^6)$ in CCSD.[27] CC2 excitation energies are only slightly inferior to those of CCSD. However, the performance of low order CC theories degrades quickly when the ground state deviates from a single reference description. Thus, these theories should be used only for spectroscopic predictions near the equilibrium geometry of molecules well described by a single reference. The inclusion of higher order excitations, such as CCSDT (or the cheaper CC3),[28] can help to recover some static correlation. Nevertheless, the accuracy of such single reference methods is further compromised if the excited states are multiconfigurational in nature. Taking the example of C_2, there remains a deviation of 0.4 and 0.85 eV in the calculated excitation energies from full configuration interaction results at the CCSDT and CC3 levels of theory, respectively.[29,30] The spin-flip approach introduced by Krylov[31,32] provides one route forward within CC theory to deal with molecules that have near degeneracies. In brief, the model employs a high spin reference state that is well-represented by a single determinant while the target states are described as spin-flipping excitations from the reference state. The success of this model has been attributed to a balanced treatment of the targeted states.

Nevertheless, a multiconfigurational starting point for inclusion of electron correlation is still required in situations where the electronic structure is complex, e.g., in atoms with open shells such as transition metals, molecules with weakly coupled electrons such as diradicals, and photodissociation. The treatment of these quasi-degenerate effects (static correlation) can be handled using the complete active space self-consistent field (CASSCF)[33,34] or the less costly restricted active space self-consistent field (RASSCF)[35] methods to obtain a qualitatively adequate description of the wave function. Subsequently, the dynamic electron correlation component can be recovered using second-order perturbation theory (CASPT2[36,37] or RASPT2[38]), and calculations performed with these methods ($O(N^5)$ scaling) generally yield excitation energies within 0.2 eV of experimental values for organic molecules.[39,40] The method has also enjoyed success in inorganic spectroscopic studies involving transition metals.[41−43] Alternatively, multireference singles and doubles configuration interaction (MRSDCI) may be used to treat dynamic electron correlation effects. The reference configurations may be taken entirely from the preceding CASSCF calculation or individually selected on the basis of their contribution to the overall wave function. Just as the lowest root corresponds to the electronic ground state in the diagonalization of the CI Hamiltonian matrix, so the higher roots are associated with the electronically excited states. The accuracy of this approach has been demonstrated for small- and medium-sized molecules[44] even though a significant drawback of the method lies in its conventionally high computational cost ($O(N^6)$).

To lower the overall cost and extend the approach to larger molecules, local correlation has been implemented within several electronic structure methods such as EOM-CCSD[45,46] and CC2[47−50] for studying excited states and molecular properties. For electronic excitations that are localized in nature (i.e., not charge-transfer type excitations), it was found to be advantageous to define an excitation domain[45] that may be predetermined via a less costly calculation, e.g., CIS. In addition, double excitations from localized occupied orbitals are segregated into strong and weak pairs, and computational savings may be derived by restricting explicit correlation of electrons to those within the strong pairs. In both the local EOM-CCSD and CC2 implementations, the calculated excitation energies for a range of medium-sized organic molecules (such as propanamide and tyrosine) were found to differ from the nonlocal calculations by less than 0.2 eV.[45−47]

Thus far, MRSDCI algorithms have been constructed within a local correlation framework (LMRSDCI) only for ground electronic states.[51−56] Here, we extend our LMRSDCI method to the treatment of valence excited states. A modified Davidson diagonalization (DD) scheme[57−60] is used in a preliminary step to obtain a refined guess for the wave function of the targeted excited state without explicitly solving for the lower roots. Once an approximate wave function is available, residual minimization via the residual minimization method−direct inversion in iterative subspace (RMM-DIIS)[61−66] scheme is used for final convergence. Using this protocol, we verify its efficacy for vertical excitation energies within LMRSDCI for various molecules (containing up to nine heavy atoms). In most cases, agreement to within 0.2 eV of nonlocal MRSDCI values is obtained. After completing this verification for the size of molecules for which nonlocal MRSDCI excitation energies are still calculable, we then use our LMRSDCI theory to predict excitation energies in some large molecules for which conventional MRSDCI could not be carried out.

2. Theory

2.1. Local Correlation within Configuration Interaction. Configuration interaction is one of the earliest methods used to account for the effects of electron correlation. The variational electronic wave function is written as a linear combination of Slater determinants (or spin-adapted configuration state functions (CSFs)) constructed from molecular orbitals.

$$\Psi^{\mathrm{CI}} = \sum_{R} c_R \Psi_R + \sum_{i,a} c_i^a \Psi_i^a + \sum_{ij,ab} c_{ij}^{ab} \Psi_{ij}^{ab} + \ldots \quad (1)$$

where $\{\Psi_R\}$ contains the set of reference configurations while $\{\Psi_i^a\}$ and $\{\Psi_{ij}^{ab}\}$ are singly and doubly excited configurations generated by promoting electrons in the reference configurations from internal orbitals $\{i,j\}$ to external orbitals $\{a,b\}$, respectively. A full CI calculation that includes all possible levels of excitations is not computationally feasible due to the prohibitive cost. As such, truncation of the CI basis is usually imposed at the level of double excitations since configurations generated from higher order excitations are not coupled directly to the reference wave function via the full Hamiltonian.[67,68] The length of the CI expansion in eq 1 may be reduced further by working within a local correlation framework that exploits the short-ranged nature of electron correlation. Using localized orbitals to span the occupied and virtual subspace, the correlated electron pairs are restricted to those in which the occupied orbitals i and j are spatially close.[51] Similarly, a correlation domain for some occupied orbital i can be imposed to consist only of virtual orbitals that are localized in the vicinity of i.[51] Variational minimization of the CI energy with respect to the CI expansion coefficients in eq 1 leads to the usual eigenfunction−eigenvalue equation, $HC = EC$.

2.2. Excited States within CI. The lowest root of the eigenvalue problem corresponds to the molecular ground state, which can be isolated using iterative subspace projection methods like DD.[69] Information on the excited states can be similarly obtained from the higher lying roots, and adaptations of DD (e.g., the Davidson−Liu method[70]) are often used for this purpose. These implementations typically require the concurrent extraction of several lower lying roots or explicit orthogonalization to the lower roots, which in turn have to be found. Since diagonalization of the CI Hamiltonian matrix constitutes a major component of the overall computational cost, savings may be derived if the targeted eigenpair can be obtained in isolation. As an alternative, the targeted interior eigenvalue may be transformed and shifted to the extrema of the spectrum. The incorporation of such "shift-and-invert" methodology within DD may be accomplished by way of oblique projection techniques along with a matrix shift.[57−60] In the conventional implementation of DD that uses orthogonal projection, an approximate eigenvector of some large matrix A is extracted from a lower dimensional subspace, $V \equiv \{v_1, v_2, \ldots, v_n\}$ (the search space). The approximate eigenvector, $\tilde{v}$, is written as a linear combination of the search space vectors, $\{v_i\}$, which constitute an orthonormal set.

$$\tilde{v} = c_1 v_1 + c_2 v_2 + \ldots + c_n v_n \quad (2a)$$

$$A(Vc) = \tilde{\lambda}(Vc) \quad (2b)$$

where $c \equiv \{c_1, c_2, \ldots, c_n\}^T$, $\tilde{v} = Vc$, and $\tilde{\lambda}$ is the approximate eigenvalue.

The eigenvalue problem in eq 2b is underdetermined, but additional constraints are imposed via the Galerkin condition, which requires the residual $r = A\tilde{v} - \tilde{\lambda}\tilde{v}$ to be orthogonal to the test space. Within orthogonal projection, the test space is equivalent to the search space (i.e., V).

$$AVc - \tilde{\lambda}Vc \perp \{v_1, v_2, \ldots, v_n\} \quad (2c)$$

The orthogonality constraint leads to

$$V^*(A - \tilde{\lambda}I)Vc = 0 \quad (2d)$$

$$V^*AVc = \tilde{\lambda}V^*Vc = \tilde{\lambda}c \quad (2e)$$

On the other hand, the test space within oblique projection, W, is allowed to be different from the search space, V. In particular, by setting $W = AV$ and requiring that W remain an orthonormal set,[57,59,60] the corresponding Galerkin−Petrov condition is

$$AVc - \tilde{\lambda}Vc \perp W, W \equiv \{w_1, w_2, \ldots, w_n\} \quad (3a)$$

$$W^*(A - \tilde{\lambda}I)Vc = 0 \quad (3b)$$

$$V^*A^*AVc = \tilde{\lambda}V^*A^*Vc = \tilde{\lambda}W^*Vc = \tilde{\lambda}W^*A^{-1}AVc = \tilde{\lambda}W^*A^{-1}Wc \quad (3c)$$

$$W^*A^{-1}Wc = \left(\frac{1}{\tilde{\lambda}}\right)c \quad (3d)$$

The low dimensional eigenvalue problem in eq 3d, transformed and reduced to the determination of eigenpairs belonging to A^{-1} in the space of W, may be solved directly using conventional methods. $\tilde{\lambda}$ is the harmonic Ritz value,[57] and with an appropriate choice for the matrix shift, σ, $1/(\tilde{\lambda} - \sigma)$ can be transformed to the extremum of the spectrum. In our work, the modified DD scheme utilizing oblique projection along with a matrix shift is used as a preliminary step to generate a refined approximation for the wave function associated with the target eigenstate. Final convergence is achieved via residual minimization using the RMM-DIIS eigenvalue solver where the guess wave function obtained earlier now serves as the secondary input. DIIS was first developed by Pulay for accelerating SCF convergence.[61−63] Later, Wood and Zunger[64] and Hutter et al.[65] introduced RMM-DIIS for solving eigenvalue problems. Our implementation of RMM-DIIS follows the approach of Kresse.[66] To reiterate, the hybrid scheme involves two separate steps. First, a few iterations of a modified Davidson method are completed to arrive at a refined guess for the target eigenstate before it is input into the RMM-DIIS scheme for final convergence.

3. Computational Details

The ground state geometries of all molecules considered in this study were optimized within density functional theory using the hybrid B3LYP exchange-correlation functional[71] and the 6-31G** basis set. Our reported vertical excitation energies T_v do not include zero point corrections, leading to some systematic errors in comparing to measured excitation energies T_0, since ground state vibrational frequencies are usually larger than excited state ones. However, the main purpose of our work is to test the accuracy of LMRSDCI for calculating T_v compared to nonlocal MRSDCI and to demonstrate its efficacy in large molecules. When used in future applications, zero-point corrections can easily be accounted for at, e.g., the DFT-B3LYP or CASSCF level of theory.

Quasi-degeneracies are treated using state-averaged CASSCF, while dynamic electron correlation effects are taken into account by second order perturbation theory (CASPT2) and MRSDCI/LMRSDCI. These latter methods without local truncation are meant to provide benchmarks for LMRSDCI. All nonlocal calculations were carried out within the Molcas 7.2 quantum chemistry package.[72] CASSCF and CASPT2 results were obtained within Molcas using the RASSCF and CASPT2 modules, respectively. For the LMRSDCI calculations, inactive orbitals were localized using the Pipek−Mezey (PM) functional,[73] while the virtual space was spanned by localized orthogonal virtual orbitals generated using the scheme described by Subotnik et al.[74] To accelerate the convergence of the MRSDCI expansion as determined by a CI coefficient cutoff of 0.1 for the reference space, the active orbitals were segregated into strongly and weakly occupied (occupation number above 1.8 and below 0.2, respectively) and then separately localized using the PM functional within each set.[75] In addition, Cholesky vectors[76−78] were used in place of conventional two-electron integrals. The Cholesky vectors were generated via an incomplete Cholesky decomposition on the two-electron integral matrix using a decomposition threshold of 10^{-7}.

The procedure for setting up orbital domains and other details of our LMRSDCI implementation can be found in our earlier work.[79−85] In brief, a sphere is associated with each molecular orbital in which a radius and a center of charge are determined. To demarcate the extent of each sphere, a list of atoms that contribute to the molecular orbital via the Mulliken population scheme is drawn up. The center of each sphere is calculated from the weighted average of the coordinates of the contributing atoms, while the radius is determined by taking the separation between the two atoms that contribute most heavily to the molecular orbital. A radius multiplier, which functions as a scaling parameter to the radius, is assigned to each sphere. The scaled value is the effective radius of the sphere and is necessary to allow for a systematic variation of the thresholds used within the weak pairs (WP) and truncation of virtuals (TOV) approximations in our local correlation studies. For example, under the WP approximation, two orbitals are deemed to be a weak pair if their associated spheres do not overlap, i.e., the separation between the spheres as given by the distance between the centers of the spheres is larger than the sum of their individual effective radii. Similarly, under the TOV approximation, the orbital domain of an internal orbital consists of a restricted set of virtual orbitals. The permitted virtual orbitals are those whose associated spheres overlap with the sphere of the internal orbital. In our work, the spheres associated with the internal (inactive and active) and external (virtual) orbitals residing on nonheteroatoms (i.e., carbon and hydrogen) were assigned a scaling factor of 1.5 and 1.2, respectively, while spheres associated with orbitals residing on the heteroatoms were assigned a larger scaling factor of 2.0.

For ground state MRSDCI/LMRSDCI calculations, the lowest roots were extracted using regular DD, and convergence to an energy difference less than 10^{-7} Hartrees between subsequent iterations was typically reached within 30 iterations. The higher lying roots corresponding to the excited states were isolated with the modified Davidson method described earlier. The parameter for the matrix shift was obtained from the corresponding eigenvalue of the preceding CASSCF calculation. After a refined initial guess was obtained from the modified Davidson scheme, the approximate CI vector was used as an input for the ensuing RMM-DIIS eigensolver. Convergence to a residual norm below 10^{-4} in between iterations required about 20−40 iterations.

4. Results

We first evaluate the performance of using the hybrid scheme described above within LMRSDCI for characterizing the valence excited states in various organic molecules for which some experimental data are available. We then go on to make some predictions for excited states in other large molecules.

We first consider the gas phase electronic transitions involving single excitations from the π (e_{1g}, HOMO) to π^* (e_{2u}, LUMO) orbitals of benzene (D_{6h}), which have been well studied experimentally. The possible excited states are determined from the direct product $e_{1g} \otimes e_{2u}$ giving rise to $^{1,3}B_{2u}$, $^{1,3}B_{1u}$, and $^{1,3}E_{1u}$ states. The singlet states are more important due to the spin selection rule $\Delta S = 0$ in electric-dipole transitions. In our work, we do not impose symmetry on the electronic wave function. Preliminary calculations on the ground A_{1g}, excited B_{2u}, and E_{1u} states with D_{2h} symmetry (the highest order point group available within Molcas) reveal that the vertical excitation energies differ from results obtained without imposing symmetry constraints on the wave function by less than 0.15 eV. The electronic term symbols used above are retained nevertheless, as they are useful for classification purposes.

For the preliminary state-averaged CASSCF calculation, we use a valence-type [6e,6o] active space comprising the six valence π electrons distributed among the six π and π^* orbitals. For an explicit treatment of $\sigma-\pi$ correlation effects,[86−88] the inclusion of σ electrons and the corresponding orbitals into the active space is necessary, i.e., a [12e,12o] active space. This is especially relevant for the so-called "ionic" B_{1u} and E_{1u} states, and therefore we expect some errors here due to the exclusion of $\sigma-\pi$ correlation. However, our goal here is to test the local correlation approximation for excited states and not to perform the most accurate

Table 1. Vertical Excitation Energies T_v (eV) from the A_{1g} Ground State to the B_{2u} Excited State of Benzene As Predicted by Various Methods and Basis Sets

basis	CASSCF	CASPT2	MRSDCI	LMRSDCI	exptl T_0[89]
6-31G*	4.89	5.14	5.03	4.95	4.90
6-31G**	4.88	5.13	5.05	4.96	
6-31+G*	4.83	5.04	4.95	4.81	
6-31++G**	4.82	5.02	4.95	4.82	
6-311G*	4.87	5.10	5.05	4.95	
6-311+G*	4.83	5.02	4.97	4.82	

Table 2. Vertical Excitation Energies T_v (eV) from the A_{1g} Ground State to the B_{1u} Excited State of Benzene As Predicted by Various Methods and Basis Sets

basis	CASSCF	CASPT2	MRSDCI	LMRSDCI	exptl T_0[89]
6-31G*	8.10	6.80	6.90	7.08	6.20
6-31G**	8.08	6.79	6.90	7.08	
6-31+G*	7.96	6.40	6.45	6.67	
6-31++G**	7.95	6.38	6.46	6.63	
6-311G*	8.06	6.80	6.92	7.03	
6-311+G*	7.92	6.39	6.45	6.61	

Table 3. Vertical Excitation Energies T_v (eV) from the A_{1g} Ground State to the E_{1u} Excited State of Benzene As Predicted by Various Methods and Basis Sets

basis	CASSCF	CASPT2	MRSDCI	LMRSDCI	exptl T_0[89]
6-31G*	9.56	7.52	7.68	7.83	6.94
6-31G**	9.54	7.47	7.61	7.82	
6-31+G*	9.29	6.69	6.80	6.96	
6-31++G**	9.27	6.70	6.83	7.00	
6-311G*	9.41	7.45	7.64	7.80	
6-311+G*	9.26	6.74	6.82	7.01	

possible CI calculations. The calculated vertical excitation energies relative to the A_{1g} ground state are summarized in Tables 1−3.

For the lowest B_{2u} excited state, the calculated vertical excitation energies are within 0.25 eV of experimental values for all levels of theory. The fact that CASSCF results are already close to experimental values is indicative of small differential correlation effects between the ground and excited states. However, this is not the case for the remaining "ionic" states of B_{1u} and E_{1u} symmetry where the CASSCF vertical excitation energies are off from experimental values by at least 1.7 eV. Incorporation of dynamic electron correlation within CASPT2 and MRSDCI improves the overall agreement with experimental values. In addition, a more extended basis may be useful in describing the diffuse character of some excited states. The improvements in the calculated vertical excitation energies for these "ionic" states are marked when diffuse functions are included on the carbon atoms, while similar augmentation on the hydrogen atoms has little influence on the final results. In all cases, LMRSDCI vertical excitation energies are within ∼0.2 eV of MRSDCI values.

Table 4. Vertical Excitation Energies T_v (eV) for the $n_O \rightarrow \pi^*$ Transition in Molecules 1−4 Shown in Figure 2

basis/molecule	CASSCF	CASPT2	MRSDCI	LMRSDCI
		6-31G*		
1	4.43	4.49	4.50	4.59
2	3.77	3.90	3.99	4.11
3	3.73	3.75	3.82	4.01
4	3.68	3.67	3.72	3.90
		6-31+G*		
1	4.43	4.45	4.52	4.61
2	3.76	3.81	3.99	4.16
3	3.71	3.71	3.81	4.03
4	3.68	3.66	3.72	3.95
		6-311G*		
1	4.42	4.47	4.52	4.61
2	3.74	3.86	4.01	4.12
3	3.71	3.71	3.80	3.95
4	3.65	3.61	3.74	3.93
		6-311+G*		
1	4.39	4.44	4.55	4.66
2	3.69	3.80	4.02	4.11
3	3.67	3.66	3.84	4.01
4	3.63	3.57	3.72	3.95

In the following series of ketone molecules, 1−4 (Figure 1), the electronic transition arising from an excitation of an electron in one of the nonbonding lone pairs on the oxygen atom into the π^* system ($n_O \rightarrow \pi^*$) is studied. For each molecule, the active space consists of the oxygen lone pair and the π electrons distributed among the π and π^* system. Moving across the series from 1 to 4, there should be a concomitant decrease in the vertical excitation energies as the π^* system is stabilized due to conjugation effects. This is captured in the calculated vertical excitation energies, which are listed in Table 4. In all cases, there is good agreement between CASPT2 and MRSDCI values while LMRSDCI results are within 0.25 eV of MRSDCI values.

The nature of excited states in nucleic acid bases, like cytosine, is of interest because these molecules are the

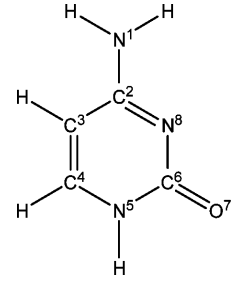

Figure 2. Cytosine, a nucleic acid base.

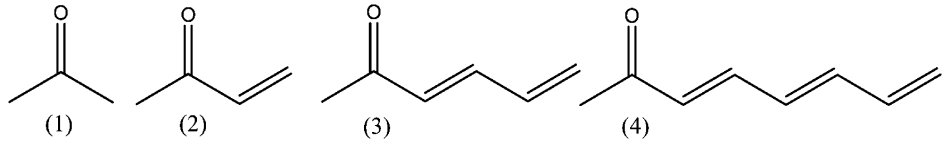

Figure 1. Test set for the study of vertical excitation energies corresponding to the $n_O \rightarrow \pi^*$ transition. The experimentally determined vertical excitation energy T_0 for molecule 1 is 4.49 eV.[90]

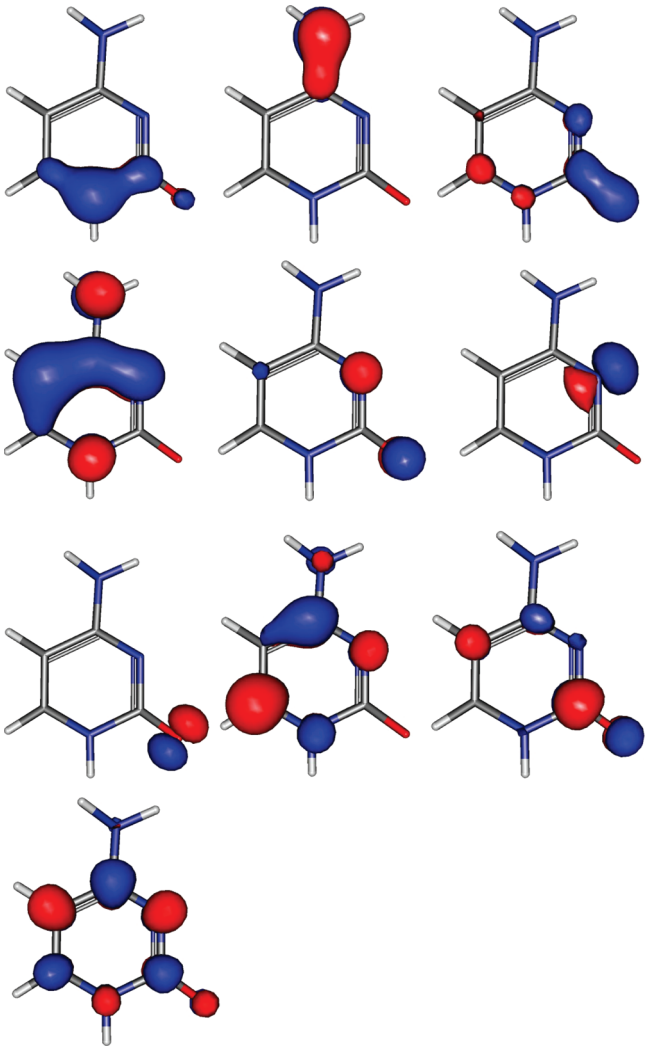

Figure 3. Active orbitals of cytosine.

Table 5. Vertical Excitation Energies T_v (eV) for the $\pi \rightarrow \pi^*$ Transition in Cytosine

basis	CASSCF	CASPT2	MRSDCI	LMRSDCI	exptl T_0[91,92]
6-31G*	5.02	4.86	4.92	5.08	4.60
6-31+G*	4.93	4.77	4.85	5.02	
6-311G*	5.03	4.87	4.92	5.10	
6-311+G*	4.92	4.70	4.86	5.02	

primary chromophores that absorb UV radiation, leading to DNA damage. The ground state molecular structure of cytosine (Figure 2) is almost planar, with the exception of the pyramidal nitrogen atom N1. For the preliminary state-averaged CASSCF calculations, the choice of active space comprised 14 electrons distributed among 10 orbitals (10 π orbitals and two lone pair orbitals situated on N8 and O7 in Figure 3). State averaging of the CASSCF calculation was performed over the ground state and the three valence excited states with equal weights. The calculated first excited state at the CASSCF level is a $\pi \rightarrow \pi^*$ state followed by $n_O \rightarrow \pi^*$ and $n_N \rightarrow \pi^*$ excited states involving the lone pair orbitals on the heteroatoms. Tables 5−7 summarize the calculated vertical excitation energies relative to the electronic ground state, in which we see that the energetic ordering of the excited states is already reproduced at the CASSCF level

Table 6. Vertical Excitation Energies T_v (eV) for the $n_O \rightarrow \pi^*$ Transition in Cytosine[a]

basis	CASSCF	CASPT2	MRSDCI	LMRSDCI
6-31G*	5.36	5.13	5.05	5.28
6-31+G*	5.21	4.95	4.99	5.18
6-311G*	5.34	5.11	5.08	5.30
6-311+G*	5.20	4.94	5.01	5.18

[a] The experimental vertical excitation energy for this transition is not available.

Table 7. Vertical Excitation Energies T_v (eV) for the $n_N \rightarrow \pi^*$ Transition in Cytosine

basis	CASSCF	CASPT2	MRSDCI	LMRSDCI	exptl T_0[91,92]
6-31G*	5.75	5.65	5.56	5.90	5.20
6-31+G*	5.70	5.50	5.45	5.85	
6-311G*	5.75	5.66	5.55	5.93	
6-311+G*	5.71	5.49	5.48	5.82	

for the two excitation energies that have been measured. The vertical excitation energies calculated at the MRSDCI and LMRSDCI levels for $\pi \rightarrow \pi^*$ and $n_O \rightarrow \pi^*$ typically agree to within 0.2 eV, but the agreement degrades to about 0.4 eV for the $n_N \rightarrow \pi^*$ state. A balanced treatment of differential electron correlation effects is necessary for the evaluation of reliable vertical excitation energies, and a larger correlation domain may be necessary in this instance. Compared to the 2p lone pair on O7, the lone pair on N8 has more 2s character and therefore may be more localized by virtue of being more tightly bound. There is then a greater change for the electron in N8 when going from the sp^2 lone pair to a more delocalized π^* orbital.

Using a larger correlation domain for both the 2sp and π^* orbitals could give a more balanced treatment in this instance, and we explore the effect of varying the local truncation parameters (radius multipliers) on the calculated vertical excitation energies using the 6-31+G* basis. The results are summarized in Table 8, which also contains the computational time, average domain size, and the total number of CSFs for each calculation. While the calculated vertical excitation energies are largely in line with values reported in the earlier tables, a significant improvement is seen for the $n_N \rightarrow \pi^*$ state when less restrictive cutoffs are used for the active orbitals (second column in Table 8) and the discrepancy between MRSDCI and LMRSDCI vertical excitation energies narrows to 0.17 eV. Further inclusion of more correlated electron pairs along with the expansion of the correlation domain (third and fourth column in Table 8) leads to even closer agreement between the MRSDCI and LMRSDCI values, but this is at the expense of higher computational cost.

Finally, we apply our LMRSDCI approach to study the $n_O \rightarrow \pi^*$ transition in $C_{18}H_{36}O$ (Figure 4), which is too costly for a nonlocal MRSDCI treatment. The active space comprises four electrons (nonbonding lone pair on oxygen + two π electrons) distributed among three orbitals (p orbital on oxygen + π and π^* orbitals). The vertical excitation energies are listed in Table 9. The localized nature of the $n_O \rightarrow \pi^*$ excitation within $C_{18}H_{36}O$ is similar to that of acetone, and the calculated vertical excitation energies in these two cases are comparable (cf. Table 4).

Table 8. Vertical Excitation Energies T_v (eV) in Cytosine Using a 6-31+G* Basis As a Function of Local Truncation Parameters[a]

excitation	MRSDCI	LMRSDCI[b]	LMRSDCI[c]	LMRSDCI[d]
$\pi\rightarrow\pi^*$	4.85 (288, 122, 5693419)	5.02 (0.12, 0.45, 0.04)	4.97 (0.42, 0.56, 0.20)	4.93 (0.52, 0.74, 0.46)
$n_O\rightarrow\pi^*$	4.99 (321, 122, 6631128)	5.16 (0.18, 0.45, 0.07)	5.12 (0.44, 0.56, 0.22)	5.11 (0.55, 0.74, 0.48)
$n_N\rightarrow\pi^*$	5.45 (305, 122, 6174262)	5.62 (0.18, 0.45, 0.07)	5.58 (0.46, 0.56, 0.24)	5.56 (0.59, 0.74, 0.51)

[a] The CPU time (hours), average domain size, and number of CSFs, respectively, are given in parentheses within the first column. For subsequent columns, the values in parentheses are expressed as a ratio of the corresponding values in the first column. Radius multipliers used for spheres associated with different orbitals are listed in the following order: Inactive, active, virtual, and orbitals residing on heteroatoms. [b] 1.5, 2.0, 1.2, and 3.0. [c] 2.0, 2.0, 1.2 and 3.0. [d] 2.0, 2.0, 2.0 and 3.0.

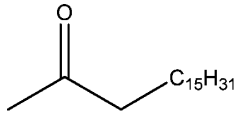

Figure 4. $C_{18}H_{36}O$, a test molecule to study the $n_O\rightarrow\pi^*$ transition using our LMRSDCI approach.

Table 9. Vertical Excitation Energies T_v (eV) for the $n_O\rightarrow\pi^*$ Transition in $C_{18}H_{36}O$

basis	CASSCF	LMRSDCI
6-31G*	4.51	4.62
6-31+G*	4.46	4.68
6-311G*	4.49	4.61
6-311+G*	4.47	4.70

5. Conclusions

We have investigated here whether local configuration interaction techniques can be used not only for ground states but also for excited states. To this end, we have extended our LMRSDCI method to solve for excited states and then evaluated valence excited states in organic molecules using LMRSDCI. To isolate the interior eigenvalues associated with the excited states of interest, a two-pronged approach was followed. First, the interior eigenvalues are transformed and shifted to the extrema of the spectrum using oblique projection along with a matrix shift within Davidson diagonalization. In this way, we obtain a refined guess for the wave function without solving for the lower roots. Subsequently, residual minimization via the RMM-DIIS method is used for final convergence toward the eigenstate of interest. In most cases, calculated vertical excitation energies within LMRSDCI are within 0.2 eV or better of MRSDCI values, suggesting that good estimates for excited state energetics in large molecules can be obtained with this method, provided that the excitation is fairly localized in nature. Working under the premise of local correlation, we expect that the LMRSDCI approach will be less reliable for excited states that are inherently diffuse (e.g., Rydberg states) and long-ranged in nature (e.g., charge transfer states). However, charge transfer processes that are spatially less extended should be treatable, since the local truncation parameters such as the radius multipliers used in our work may be tuned so that they are large enough to include excitations to/from nearest neighbors. This would allow us to study the shorter-ranged charge transfer processes that would remain a challenge for TDDFT.

We must note in closing that if a large active space is required to model the physical problem, the preceding CASSCF calculation can become the overall bottleneck for the entire calculation, which will limit the applicability of our method. Although the EOM-CC and LR-CC theories do not suffer from this limitation, current low order implementations of these latter methods remain most suitable for describing single electron excitations from ground to excited states that are separately well-described using a single configuration. Multireference methods such as the one presented here are still necessary for all phenomena and molecules in which near-degeneracies appear.

Acknowledgment. We are grateful to the National Science Foundation for support of this work. One of the authors (T.S.C) thanks the Agency for Science, Technology and Research A*STAR for funding. We also thank Dr. Johannes Hachmann for pointing out his very helpful related work to us at the beginning of this project.

References

(1) Kraemer, K. H. *Proc. Natl. Acad. Sci. U.S.A.* **1997**, *94*, 11.

(2) Mukhtar, H.; Elmets, C. A. *Photochem. Photobiol.* **1996**, *63*, 355.

(3) Head-Gordon, M.; Rico, R. J.; Oumi, M.; Lee, T. J. *Chem. Phys. Lett.* **1994**, *219*, 21.

(4) Grafia, A. M.; Lee, T. J.; Head-Gordon, M. *J. Phys. Chem.* **1995**, *99*, 3493.

(5) Krylov, A. I. *Chem. Phys. Lett.* **2001**, *350*, 522.

(6) Maurice, D.; Head-Gordon, M. *J. Phys. Chem.* **1996**, *100*, 6131.

(7) Casanova, D.; Head-Gordon, M. *J. Chem. Phys.* **2008**, *129*, 064104.

(8) Runge, E.; Gross, E. K. U. *Phys. Rev.* **1984**, *136*, B864.

(9) Marques, M. A. L. Time-Dependent Density Functional Theory. In *Lecture Notes in Physics*; Ullrich, C., Nogueira, F., Rubio, A., Gross, E. K. U., Eds.; Springer: Berlin, 2006; Vol. 706, pp 323.

(10) Tozer, D. J.; Amos, R. D.; Handy, N. C.; Roos, B. O. *Mol. Phys.* **1999**, *97*, 859.

(11) Dreuw, A.; Head-Gordon, M. *J. Am. Chem. Soc.* **2004**, *126*, 4007.

(12) Dreuw, A.; Head-Gordon, M. *Chem. Rev.* **2005**, *105*, 4009.

(13) Casida, M. E. *THEOCHEM* **2009**, *914*, 3.

(14) Wu, Q.; Van Voorhis, T. *Phys. Rev. A* **2005**, *72*, 024502.

(15) Wu, Q.; Van Voorhis, T. *J. Chem. Theory Comput.* **2006**, *2*, 765.

(16) Wu, Q.; Van Voorhis, T. *J. Chem. Phys.* **2006**, *125*, 164105.

(17) Geertsen, J.; Rittby, M.; Bartlett, R. J. *Chem. Phys. Lett.* **1989**, *164*, 57.

(18) Stanton, J. F.; Bartlett, R. J. *J. Chem. Phys.* **1993**, *98*, 7029.

(19) Monkhorst, H. J. *Int. J. Quantum Chem. Symp.* **1977**, *11*, 421.

(20) Dalgaard, E.; Monkhorst, H. J. *Phys. Rev. A* **1983**, *28*, 1217.

(21) Koch, H.; Jørgensen, P. *J. Chem. Phys.* **1990**, *93*, 3333.

(22) Noga, J.; Bartlett, R. J. *J. Chem. Phys.* **1987**, *86*, 7041.

(23) Scuseria, G. E.; Schaefer, H. F., III. *Chem. Phys. Lett.* **1988**, *152*, 382.

(24) Oliphant, N.; Adamowicz, L. *J. Chem. Phys.* **1992**, *95*, 6645.

(25) Kucharski, S. A.; Bartlett, R. J. *J. Chem. Phys.* **1992**, *97*, 4282.

(26) Christiansen, O.; Koch, H.; Jørgensen, P. *Chem. Phys. Lett.* **1995**, *243*, 409.

(27) Purvis, G. D., III; Bartlett, R. J. *J. Chem. Phys.* **1982**, *76*, 1910.

(28) Koch, H.; Christiansen, O.; Jørgensen, P.; Sanchez de Merás, A. M.; Helgaker, T. J. *Chem. Phys.* **1997**, *106*, 1808.

(29) Hirata, S. *J. Chem. Phys.* **2004**, *121*, 244106.

(30) Christiansen, O.; Koch, H.; Jørgensen, P.; Olsen, P. J. *Chem. Phys. Lett.* **1996**, *256*, 185.

(31) Krylov, A. I. *Chem. Phys. Lett.* **2001**, *338*, 375.

(32) Krylov, A. I. *Acc. Chem. Res.* **2006**, *39*, 83.

(33) Roos, B. O.; Taylor, P. R. *Chem. Phys.* **1980**, *48*, 157.

(34) Roos, B. O. *Adv. Chem. Phys.* **1987**, *69*, 399.

(35) Malmqvist, P. A.; Rendell, A.; Roos, B. O. *J. Phys. Chem.* **1990**, *94*, 5477.

(36) Andersson, K.; Malmqvist, P. A.; Roos, B. O.; Sadlej, A. J.; Wolinski, K. *J. Phys. Chem.* **1990**, *94*, 5483.

(37) Anderson, K.; Malmqvist, P. A.; Roos, B. O. *J. Chem. Phys.* **1992**, *96*, 1218.

(38) Malmqvist, P. A.; Pierloot, K.; Shahi, A. R. M.; Cramer, C. J.; Gagliardi, L. *J. Chem. Phys.* **2008**, *128*, 204109.

(39) Serrano-Andrés, L.; Merchán, M.; Nebot-Gil, I.; Lindh, R.; Roos, B. O. *J. Chem. Phys.* **1993**, *98*, 3151.

(40) Roos, B. O.; Serano-Andrés, L.; Merchán, M. *Pure Appl. Chem.* **1993**, *65*, 1693.

(41) Roos, B. O.; Fülscher, M. P.; Malmqvist, P. A.; Merchán, M.; Serrano-Andrés, L. In *Quantum Mechanical Electronic Structure Calculations with Chemical Accuracy*; Langhoff, S. R., Eds.; Kluwer Academic Publishers: Dordrecht, The Netherlands, 1995; pp 357.

(42) Pierloot, K. *Mol. Phys.* **2003**, *101*, 2083.

(43) Malmqvist, P. A.; Pierloot, K.; Rehaman Moughal Shahi, A.; Cramer, C. J.; Gagliardi, L. *J. Chem. Phys.* **2008**, *128*, 204109.

(44) Partridge, H.; Langhoff, S. R.; Bauschlicher, C. W., Jr. In *Quantum Mechanical Electronic Structure Calculations with Chemical Accuracy*; Langhoff, S. R., Eds.; Kluwer Academic Publishers: Dordrecht, The Netherlands, 1995; pp 209.

(45) Korona, T.; Werner, H.-J. *J. Chem. Phys.* **2003**, *118*, 3006.

(46) Crawford, T. D.; King, R. A. *Chem. Phys. Lett.* **2002**, *366*, 611.

(47) Kats, D.; Korona, T.; Schütz, M. *J. Chem. Phys.* **2006**, *125*, 104106.

(48) Kats, D.; Korona, T.; Schütz, M. *J. Chem. Phys.* **2007**, *127*, 064107.

(49) Kats, D.; Schütz, M. *J. Chem. Phys.* **2009**, *131*, 124117.

(50) Kats, D.; Schütz, M. *Z. Phys. Chem.* **2010**, *224*, 601.

(51) Pulay, P. *Chem. Phys. Lett.* **1983**, *100*, 151.

(52) Saebø, S.; Pulay, P. *Chem. Phys. Lett.* **1985**, *113*, 13.

(53) Pulay, P.; Saebø, S. *Theor. Chim. Acta* **1986**, *69*, 357.

(54) Saebø, S.; Pulay, P. *J. Chem. Phys.* **1987**, *86*, 914.

(55) Saebø, S.; Pulay, P. *J. Chem. Phys.* **1988**, *88*, 1884.

(56) Saebø, S.; Pulay, P. *Annu. Rev. Phys. Chem.* **1993**, *44*, 213.

(57) Paige, C. C.; Parlett, B. N.; van der Vorst, H. A. *Numer. Linear Algebra Appl.* **1995**, *2*, 115.

(58) Morgan, R. B. *Linear Algebra Appl.* **1991**, *154*, 289 (1991).

(59) Sleijpen, G. L. G.; van der Vorst, H. A. *SIAM J. Matrix Anal. Appl.* **1996**, *17*, 401.

(60) Dorando, J. J.; Hachmann, J.; Chan, G. K.-L. *J. Chem. Phys.* **2007**, *127*, 084109.

(61) Pulay, P. *Chem. Phys. Lett.* **1980**, *73*, 393.

(62) Pulay, P. *J. Comput. Chem.* **1982**, *3*, 556.

(63) Csaszar, P.; Pulay, P. *J. Mol. Struct.* **1984**, *114*, 31.

(64) Wood, D. M.; Zunger, A. *J. Phys. A: Math. Gen.* **1985**, *18*, 1343.

(65) Hutter, J.; Lüthi, H. P.; Parrinello, M. *Comput. Mater. Sci.* **1994**, *2*, 244.

(66) Kresse, G.; Furthmuller, J. *Phys. Rev. B* **1996**, *54*, 11169.

(67) Whitten, J. L.; Hackmeyer, M. *J. Chem. Phys.* **1969**, *51*, 5584.

(68) Peyerimhoff, D.; Buenker, J. *Chem. Phys. Lett.* **1972**, *16*, 235.

(69) Davidson, E. R. *J. Comput. Phys.* **1975**, *17*, 87.

(70) Liu, B. *Numerical Algorithm in Chemistry: Algebraic Methods*; LBL-8158, UC-32, CONF-780878; National Resource for Computation in Chemistry, Lawrence Berkeley Laboratory: Berkeley, California, 1978; pp 49.

(71) Becke, A. D. *J. Chem. Phys.* **1993**, *98*, 1372.

(72) Aquilante, F.; De Vico, L.; Ferré, N.; Ghigo, G.; Malmqvist, P. A.; Neogrády, P.; Pedersen, T. B.; Pitoňák, M.; Reiher, M.; Roos, B. O.; Serrano-Andrés, L.; Urban, M.; Veryazov, V.; Lindh, R. *J. Comput. Chem.* **2009**, *31*, 224.

(73) Pipek, J.; Mezey, P. G. *J. Chem. Phys.* **1989**, *90*, 4916.

(74) Subotnik, J. E.; Dutoi, A. D.; Head-Gordon, M. *J. Chem. Phys.* **2005**, *123*, 114108.

(75) Bytautas, L.; Ivanic, J.; Ruedenberg, K. *J. Chem. Phys.* **2003**, *119*, 8217.

(76) Beebe, N. H. F.; Linderberg, J. *Int. J. Quantum Chem.* **1977**, *12*, 683.

(77) Røeggen, I.; Wisløff-Nielsen, E. *Chem. Phys. Lett.* **1986**, *132*, 154.

(78) O'Neal, D. W.; Simons, J. *Int. J. Quantum Chem.* **1989**, *36*, 673.

(79) Reynolds, G.; Martinez, T. J.; Carter, E. A. *J. Chem. Phys.* **1996**, *105*, 6455.

(80) Reynolds, G.; Carter, E. A. *Chem. Phys. Lett.* **1997**, *265*, 660.

(81) Walter, D.; Carter, E. A. *Chem. Phys. Lett.* **2001**, *346*, 177.

(82) Walter, D.; Szilva, A. B.; Niedfeldt, K.; Carter, E. A. *J. Chem. Phys.* **2002**, *117*, 1982.

(83) Walter, D.; Venkatnathan, A.; Carter, E. A. *J. Chem. Phys.* **2003**, *118*, 8127.

(84) Chwee, T. S.; Szilva, A. B.; Lindh, R.; Carter, E. A. *J. Chem. Phys.* **2008**, *128*, 224106.

(85) Chwee, T. S.; Carter, E. A. *J. Chem. Phys.* **2010**, *132*, 074104.

(86) Malmqvist, P. A.; Roos, B. O.; Fülscher, M. P.; Rendell, A. *Chem. Phys.* **1992**, *162*, 359.

(87) Roos, B. O.; Andersson, K.; Fülscher, M. P. *Chem. Phys. Lett.* **1992**, *192*, 5.

(88) Angeli, C. *J. Comput. Chem.* **2009**, *30*, 1319.

(89) Hiraya, A.; Shobatake, K. *J. Chem. Phys.* **1991**, *94*, 7700.

(90) Mulliken, R. S. *J. Chem. Phys.* **1935**, *8*, 564.

(91) Clark, L. B.; Peschel, G. G.; Tinoco, I. *J. Phys. Chem.* **1965**, *69*, 3615.

(92) Clark, L. B.; Tinoco, I. *J. Am. Chem. Soc.* **1965**, *87*, 11.

CT100486Q